

## E<sup>n</sup>GFP: protein nanodevices tailored for intracellular biosensing

Owing to their genetically encoded fluorescence, green fluorescent proteins (GFPs) have become an invaluable tool for the optical labeling and tracking of protein molecules in living cells at high spatial and temporal resolution. One of the ultimate challenges in microscopy is to devise GFP-based biosensors that combine the high resolution imaging property of luminescent probes with the functional information afforded by biochemical analysis. Here we present the development of new GFP-based biosensors for high-resolution intracellular pH and chloride sensing. The spectral properties of the E<sup>n</sup>GFP class (F64L/T203Y) were exploited for the design of a multiplex pH and chloride sensor, which overcame the limitations of existing methods to sense intracellular chloride concentration and pH.

### E<sup>1</sup>GFP as targeted biosensor of intracellular pH

The chromophore of E<sup>n</sup>GFP can exist in two optically distinguished forms (neutral and anionic) that are both fluorescent.<sup>1,2</sup> Such a dual fluorescence property makes possible the fabrication of ratiometric (i.e. concentration independent) pH sensors tailored to the 5-9 pH range.<sup>3,4</sup>

Intracellular pH (pH<sub>i</sub>) is a remarkable modulator of cell structure and function.<sup>4</sup> The genetically-encoded nature of GFP-pH<sub>i</sub> biosensors makes them the perfect fluorescent nanoreporters of intracellular H<sup>+</sup> concentration. In this field, we developed new E<sup>1</sup>GFP-based pH biosensor ratiometric by emission when excited at 405 nm (Fig. 1a), denoted as E<sup>1</sup>GFP (F64L/T203Y GFP).<sup>1</sup> By careful selection of the emission ranges in the ratiometric ratio, the working pH interval of E<sup>1</sup>GFP can be tuned from 6.0 up to neutrality, as displayed both *in vitro* and in cultured cells clamped to different pH values (Fig. 1b and d).<sup>4</sup> We demonstrated the ability of E<sup>1</sup>GFP to report dynamically on the pH of cell components by following the caveolin trafficking in the cell (Fig. 1e) and the gradual endosomal acidification associated with HIV Tat86 (fused to E<sup>1</sup>GFP) cell internalization.<sup>5</sup> The measurement of pH in endocytic vesicles is a way to monitor the progression of internalized exogenous molecules from their binding to receptors on the cell membrane down to their processing in specific cell compartments. After 4h Tat-E<sup>1</sup>GFP-stained

vesicles onto the plasma membrane showed a nearly neutral pH value, owing to their contact with the external buffer (Fig. 1f), whereas in the internalized pool we identified two endosomal subpopulations with two different pH values: ~6.5 and ~5.9 (Fig. 1f).<sup>4</sup> After 6h, the pH of each compartment significantly decreased. These findings are consistent with a gradual acidification associated with Tat internalization, indicating a prevalent endocytic mechanism of uptake.

### Simultaneous intracellular pH and chloride concentration measurements

Interestingly, the S65T mutation introduces a specific anion-binding site in E<sup>n</sup>GFP.<sup>4</sup> We thus decided to exploit this peculiarity in the development of a novel chloride sensor. Indeed Cl<sup>-</sup> participates in many physiological functions including stabilization of neuronal resting potential, charge balance in vesicular acidification, and regulation of cell volume.<sup>10</sup> Yet, processes regulating intracellular chloride concentration, [Cl<sup>-</sup>]<sub>i</sub>, are still widely unexplored mainly as a consequence of limiting methods to quantify chloride fluxes in living cells.

Our sensor was conceived as ratiometric, genetically-encoded and capable to simultaneously measure [Cl<sup>-</sup>]<sub>i</sub> and pH<sub>i</sub>. So, DsRed-monomer, which is insensitive to chloride and pH, was fused to E<sup>2</sup>GFP via a peptide linker as illustrated in Fig. 2A. The proposed sensor *in vitro* reversible (sub-second) response to mM

Daniele Arosio

d.ariosio@sns.it

#### Collaborators

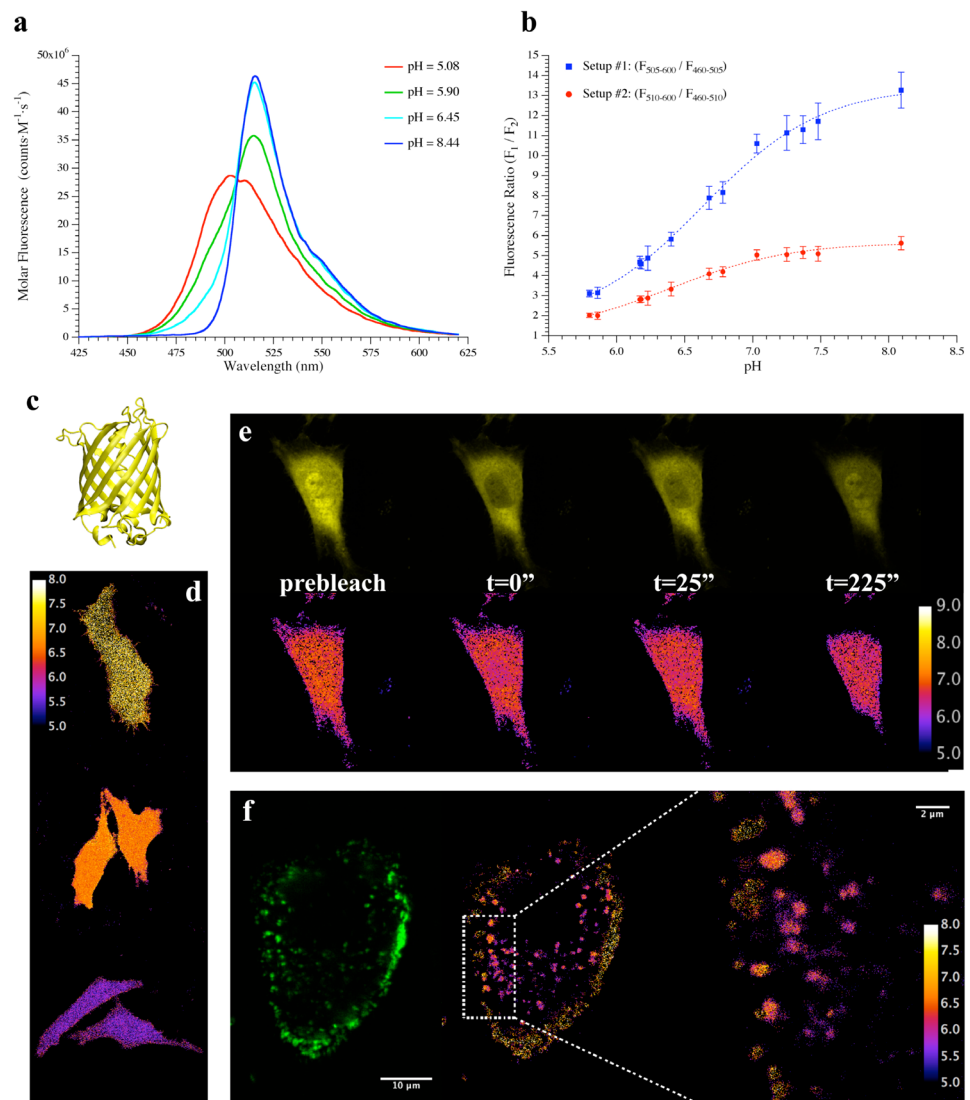
L. Albertazzi  
F. Beltram  
R. Bizzarri  
F. Cardarelli  
R. Gualdani  
S. Guidi  
S. Luin  
L. Marchetti  
R. Nifosi  
F. Ricci  
M. Serresi  
C. Viappiani

[Cl]<sub>i</sub> variation along with fast response to pH variations (< 1 ms) in the physiological pH range.<sup>3</sup> Green-to-red fluorescence ratio is regulated by [Cl]<sub>i</sub>; according to simple Langmuir isotherm (Fig. 2C) in the range from 1 to 300 mM. Subsequently, we demonstrated that the proposed sensor allows dynamic live imaging of [Cl]<sub>i</sub> in GABA-A receptor-triggered Cl<sup>-</sup> fluxes (Fig. 2C). Remarkably, by targeting the novel biosensor to the secretory pathway of neuroendocrine cells we provided an unprecedented quantification of the [Cl]<sub>i</sub> in large dense core vesicles (Fig. 2D).

The high-resolution characterization of the anion binding-site structure (Fig. 3) in E<sup>2</sup>GFP suggested further optimization of the chloride sensing GFP. Site directed mutagenesis allowed us to keenly control E<sup>n</sup>GFP chloride affinity (Fig. 3A). Remarkably, we engineered a new FP, E<sup>2</sup>GFP-V224L,<sup>11</sup> which bears the highest chloride affinity among FP. Thermodynamic and structural results together showed entropic origin of the increased chloride affinity owing to the presence of a water molecule in the binding pocket.

**Fig 1**

(a) Emission fluorescence of E<sup>1</sup>GFP at different pH by exciting at 405 nm; (b) Two ratiometric calibrations of E<sup>1</sup>GFP in HeLa cells clamped at different pH values: note that the ratiometric curve amplitude and linear range depend on the emission intervals; (c) typical b-barrel structure of E<sup>1</sup>GFP; (d) ratiometric pH maps of HeLa cells expressing E<sup>1</sup>GFP and clamped at pH 5.2 (lower panel), 6.7 (middle panel), and 8 (upper panel); (e) pH measured by E<sup>1</sup>GFP is not dependent on dynamic processes occurring in the cell: a diffusion-dependent fluorescence recovery in the nucleus is induced by bleaching (upper panel) but the measured pH is not biased by time dependent fluorescent changes (lower panel); (f) Real-time monitoring of endocytosis of Tat-E<sup>1</sup>GFP in HeLa cells at 4h: fluorescence is distributed on the cell membrane and internalized in endocytotic vesicles (left panel), whose pH is different (middle and right panel).



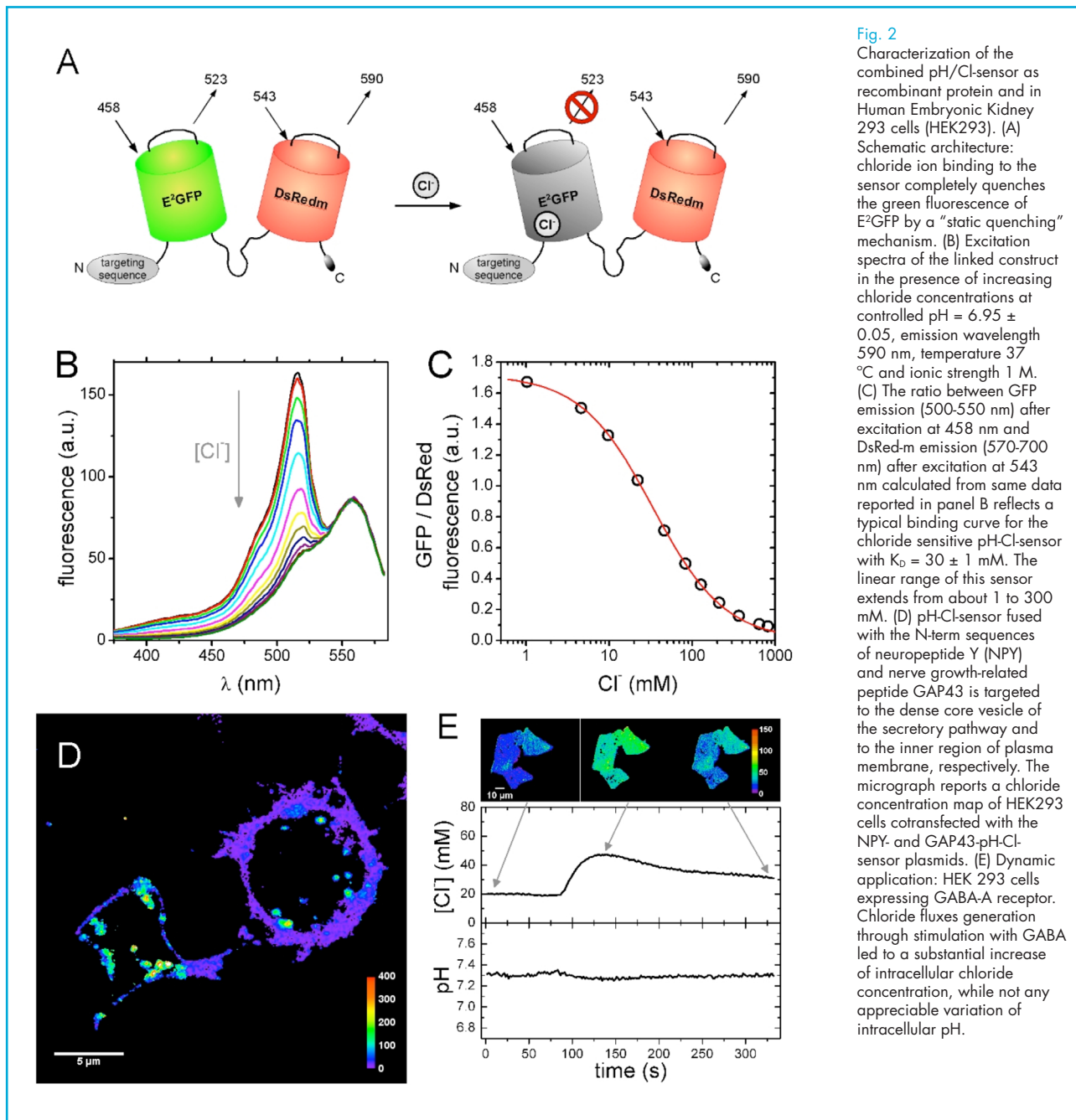


Fig. 2

Characterization of the combined pH/Cl<sup>-</sup> sensor as recombinant protein and in Human Embryonic Kidney 293 cells (HEK293). (A) Schematic architecture: chloride ion binding to the sensor completely quenches the green fluorescence of E<sup>2</sup>GFP by a "static quenching" mechanism. (B) Excitation spectra of the linked construct in the presence of increasing chloride concentrations at controlled pH = 6.95 ± 0.05, emission wavelength 590 nm, temperature 37 °C and ionic strength 1 M. (C) The ratio between GFP emission (500-550 nm) after excitation at 458 nm and DsRed-m emission (570-700 nm) after excitation at 543 nm calculated from same data reported in panel B reflects a typical binding curve for the chloride sensitive pH-Cl<sup>-</sup> sensor with K<sub>D</sub> = 30 ± 1 mM. The linear range of this sensor extends from about 1 to 300 mM. (D) pH-Cl<sup>-</sup> sensor fused with the N-term sequences of neuropeptide Y (NPY) and nerve growth-related peptide GAP43 is targeted to the dense core vesicle of the secretory pathway and to the inner region of plasma membrane, respectively. The micrograph reports a chloride concentration map of HEK293 cells cotransfected with the NPY- and GAP43-pH-Cl<sup>-</sup> sensor plasmids. (E) Dynamic application: HEK 293 cells expressing GABA-A receptor. Chloride fluxes generation through stimulation with GABA led to a substantial increase of intracellular chloride concentration, while not any appreciable variation of intracellular pH.

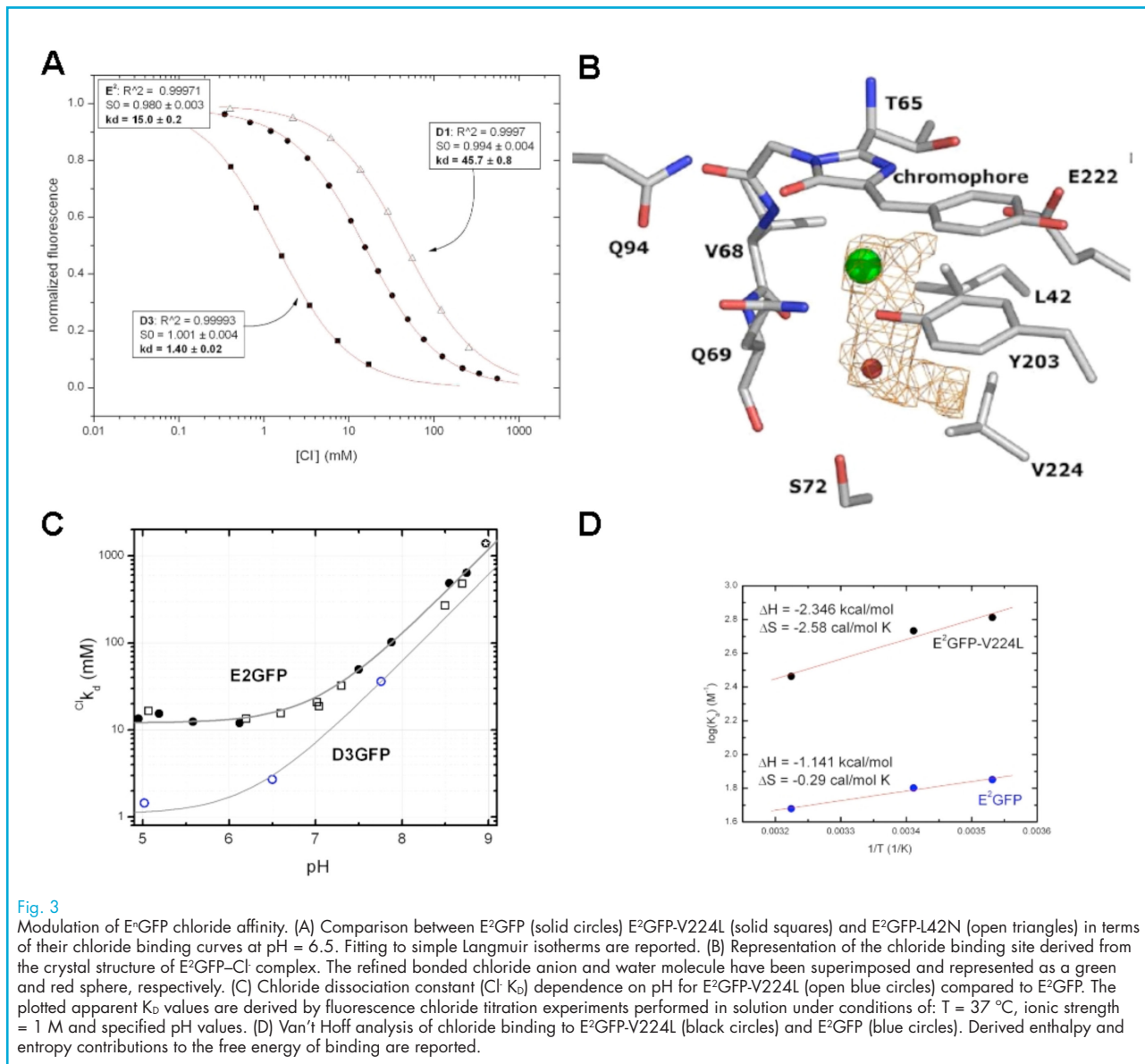


Fig. 3

Modulation of E<sup>2</sup>GFP chloride affinity. (A) Comparison between E<sup>2</sup>GFP (solid circles) E<sup>2</sup>GFP-V224L (solid squares) and E<sup>2</sup>GFP-L42N (open triangles) in terms of their chloride binding curves at pH = 6.5. Fitting to simple Langmuir isotherms are reported. (B) Representation of the chloride binding site derived from the crystal structure of E<sup>2</sup>GFP-Cl<sup>-</sup> complex. The refined bonded chloride anion and water molecule have been superimposed and represented as a green and red sphere, respectively. (C) Chloride dissociation constant (Cl<sup>-</sup> K<sub>d</sub>) dependence on pH for E<sup>2</sup>GFP-V224L (open blue circles) compared to E<sup>2</sup>GFP. The plotted apparent K<sub>d</sub> values are derived by fluorescence chloride titration experiments performed in solution under conditions of: T = 37 °C, ionic strength = 1 M and specified pH values. (D) Van't Hoff analysis of chloride binding to E<sup>2</sup>GFP-V224L (black circles) and E<sup>2</sup>GFP (blue circles). Derived enthalpy and entropy contributions to the free energy of binding are reported.

## References

- [1] Bizzarri, R.; Nifosi, R.; Abbruzzetti, S.; Rocchia, W.; Guidi, S.; Arosio, D.; Garau, G.; Campanini, B.; Grandi, E.; Ricci, F.; Viappiani, C.; Beltram, F. *Biochemistry* 2007, 46, 5494-5504.
- [2] Arosio, D.; Garau, G.; Ricci, F.; Marchetti, L.; Bizzarri, R.; Nifosi, R.; Beltram, F. *Biophys J* 2007, 93, 232-44.
- [3] Bizzarri, R.; Nifosi, R.; Abbruzzetti, S.; Rocchia, W.; Guidi, S.; Arosio, D.; Garau, G.; Campanini, B.; Grandi, E.; Ricci, F.; Viappiani, C.; Beltram, F. *Biophys. J.* 2007, 329A-329A.
- [4] Bizzarri, R.; Serresi, M.; Luin, S.; Beltram, F. *Anal Bioanal Chem* 2009, 393, 1107-1122.
- [5] Serresi, M.; Bizzarri, R.; Cardarelli, F.; Beltram, F. *Anal Bioanal Chem* 2009, 393, 1123-1133.